J|A|C|S
COMMUNICATIONS

Published on Web 06/20/2002

Size-Controlled Synthesis of Magnetite Nanoparticles

Shouheng Sun* and Hao Zeng

IBM T. J. Watson Research Center, Yorktown Heights, New York 10598

Received April 11, 2002

The synthesis of magnetite nanoparticles with controlled size has long been of scientific and technological interest. Magnetite (Fe_3O_4) is a common magnetic iron oxide that has a cubic inverse spinel structure with oxygen forming a fcc closed packing and Fe cations occupying interstitial tetrahedral sites and octahedral sites.[1] The electrons can hop between Fe^{2+} and Fe^{3+} ions in the octahedral sites at room temperature, rendering magnetite an important class of half-metallic materials.[2] Its particle dispersions have been widely used as ferrofluid in, for example, rotary shaft sealing, oscillation damping, and position sensing.[3] The use of properly coated magnetite nanoparticles in clinical medicine has also intensified. With proper surface coating, these magnetic nanoparticles can be dispersed into water, forming water-based suspensions.[4] Such a suspension can interact with an external magnetic field and be positioned to a specific area, facilitating magnetic resonance imaging for medical diagnosis[5] and AC magnetic field-assisted cancer therapy.[6] All these technological and medical applications require that the nanoparticles are superparamagnetic with sizes smaller than 20 nm and the overall particle size distribution is narrow so that the particles have uniform physical and chemical properties. However, producing magnetite particles with the desired size and acceptable size distribution without particle aggregation has consistently been a problem.

Here we report a simple organic-phase synthesis of magnetite nanoparticles with sizes variable from 3 to 20 nm in diameter. Fe_3O_4 nanoparticles are commonly produced via coprecipitation of ferrous (Fe^{2+}) and ferric (Fe^{3+}) ions by a base, usually NaOH, or $NH_3 \cdot H_2O$, in an aqueous solution,[7] or they may be made by thermal decomposition of alkaline solution of Fe^{3+} chelate in the presence of hydrazine[8] and by sonochemical decomposition of hydrolyzed Fe(II) salt followed by thermal treatment.[9] The disadvantage of these aqueous solution syntheses is that the pH value of the reaction mixture has to be adjusted in both the synthesis and purification steps, and the process toward smaller (<20 nm) monodisperse nanoparticles has only very limited success. Organic solution-phase decomposition of the iron precursor at high temperatures has been widely used in iron oxide nanoparticle synthesis. Recent advance in the synthesis has demonstrated that direct decomposition of $FeCup_3$,[10] or decomposition of $Fe(CO)_5$ followed by oxidation,[11] can lead to high quality monodisperse γ-Fe_2O_3 nanoparticles. However the synthesis of monodisperse Fe_3O_4 nanoparticles with sizes below 20 nm has not yet been reported. Here we demonstrate that high-temperature (265 °C) reaction of iron (III) acetylacetonate, $Fe(acac)_3$, in phenyl ether in the presence of alcohol, oleic acid, and oleylamine can be used to make monodisperse magnetite nanoparticles (Scheme 1). With the smaller magnetite nanoparticles as seeds, larger monodisperse magnetite nanoparticles of up to 20 nm in diameter can be synthesized and dispersed into nonpolar solvent. The process does not require a size-selection procedure and is readily scaled up for mass production.

Scheme 1

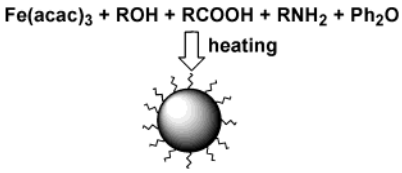

According to Scheme 1, the 4-nm Fe_3O_4 nanoparticles are made as follows:[12] $Fe(acac)_3$ (2 mmol) was mixed in phenyl ether (20 mL) with 1,2-hexadecanediol (10 mmol), oleic acid (6 mmol), and oleylamine (6 mmol) under nitrogen and was heated to reflux for 30 min. After cooled to room temperature, the dark-brown mixture was treated with ethanol under air, and a dark-brown material was precipitated from the solution. The product was dissolved in hexane in the presence of oleic acid and oleylamine and reprecipitated with ethanol to give 4-nm Fe_3O_4 nanoparticles.

To make larger Fe_3O_4 nanoparticles, a seed-mediated growth method was used. This method has been recently applied to larger metallic nanoparticle and nanocomposite synthesis[13] and is believed to be an alternative way of making monodisperse nanoparticles along with LaMer's method through fast supersaturated-burst nucleation[14] and Finke's method via slow, continuous nucleation and fast, autocatalytic surface growth.[15] In our process, the smaller Fe_3O_4 nanoparticles were mixed with more precursor materials shown in Scheme 1, and the mixture was heated as in the synthesis of 4-nm nanoparticles. By controlling the quantity of nanoparticle seeds, Fe_3O_4 nanoparticles with various sizes can be formed. For example, mixing and heating 62 mg of 8-nm Fe_3O_4 nanoparticles with 2 mmol of $Fe(acac)_3$, 10 mmol stearyl alcohol, 2 mmol of oleic acid, and 2 mmol oleylamine led to 12-nm Fe_3O_4 nanoparticles, while changing the mass of seeds into 15 mg led to 16-nm Fe_3O_4 nanoparticles. TEM analysis shows that Fe_3O_4 nanoparticles prepared according to Scheme 1 or a seed-mediated growth method are nearly monodisperse. Figure 1 shows typical TEM images from representative 16-nm Fe_3O_4 nanoparticles deposited from their dodecane dispersion on an amorphous carbon surface and dried at 60 °C for 30 min. It can be seen that particles have narrow size distribution (Figure 1A) and can form large area self-assembled superlattices (Figure 1B).

Both the high-resolution TEM (HRTEM) and X-ray diffraction (XRD) are used to obtain structure information of the Fe_3O_4 nanoparticle. The HRTEM images show that these nanoparticles are single crystalline, as indicated clearly by atomic lattice fringes (Figure 1C). Figure 2 are the XRD patterns of variously sized Fe_3O_4 nanoparticle assemblies made from Scheme 1 (Figure 2A) and seed-mediated growth (Figure 2B−D). The position and relative intensity of all diffraction peaks match well with those of the commercial magnetite powder (Aldrich catalog No. 31,006-9). The average particle diameter can be estimated using Scherrer's formula.[16] For

* To whom correspondence should be addressed. E-mail: ssun@us.ibm.com.

10.1021/ja026501x CCC: $22.00

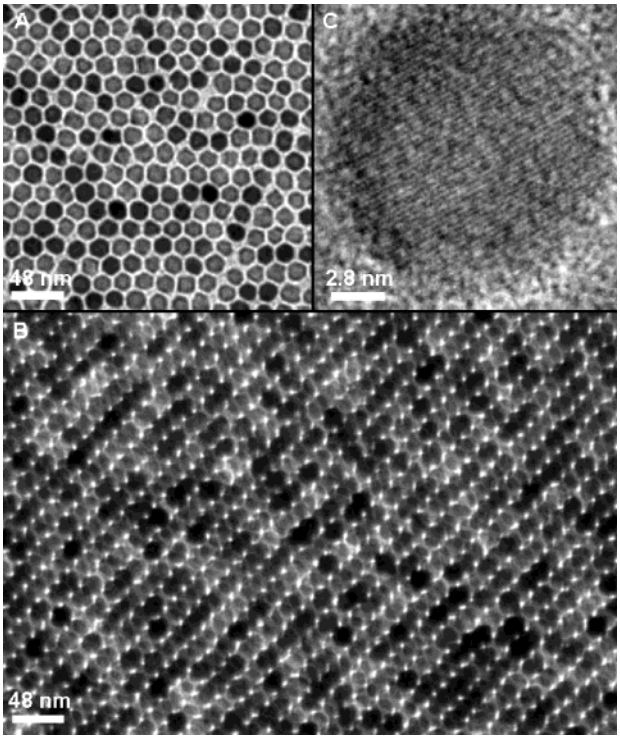

Figure 1. TEM bright field image of 16-nm Fe_3O_4 nanoparticles deposited from their dodecane dispersion on amorphous carbon surface and dried at 60 °C for 30 min: (A) a monolayer assembly, (B) a multilayer assembly, (C) HRTEM image of a single Fe_3O_4 nanoparticle. The images were acquired from a Philips EM 430 at 300 KV.

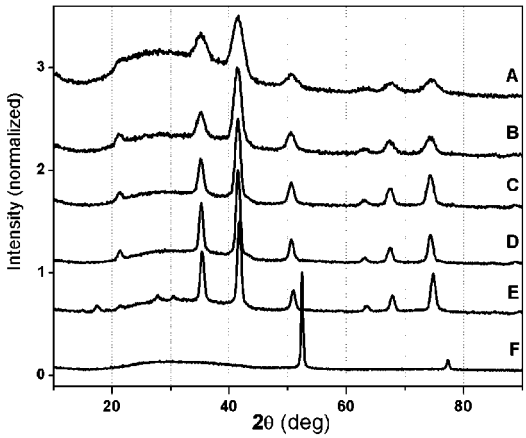

Figure 2. X-ray diffraction patterns of (A) 4-nm, (B) 8-nm, (C) 12-nm, (D) 16-nm Fe_3O_4 nanoparticle assemblies, and (E) γ-Fe_2O_3 nanoparticle assembly obtained from the oxidation of a 16-nm Fe_3O_4 nanoparticle assembly under oxygen at 250 °C for 2 h, (F) bcc-Fe nanoparticle assembly obtained from the reduction of a 16-nm Fe_3O_4 nanoparticle assembly under Ar + H_2 (5%) at 400 °C for 2 h. All samples were deposited on glass substrates from their hexane dispersions. Diffraction patterns were collected on a Simens D-500 diffractometer under Co Kα radiation (λ = 1.788965 Å)

example, the average size calculated from Figure 2D is about 15 nm, close to the 16-nm average size determined by statistical analysis of the TEM images, indicating that each individual particle is a single crystal.

The as-synthesized Fe_3O_4 nanoparticle assemblies can be transformed easily into either γ-Fe_2O_3 or α-Fe nanoparticle assemblies by annealing at different atmospheres. Figure 2E is the XRD pattern of a red-brown nanoparticle assembly obtained from O_2 oxidation of a black 16-nm Fe_3O_4 particle assembly at 250 °C. Compared to Figure 2D, the large-angle peaks in Figure 2E shift slightly to higher angles, and additional small peaks appear at lower angles. All peak positions and relative intensities match well with those of commercial γ-Fe_2O_3 powder materials (Aldrich catalog No. 48,066-5), indicating that the oxidation of Fe_3O_4 under O_2 leads to γ-Fe_2O_3. Accordingly, due to the oxidation, the saturation magnetization (σ_s) of the assembly is reduced from 82 emu/g to 70 emu/g (300 K).[17] After annealing under Ar + 5% H_2 at 400 °C, the Fe_3O_4 nanoparticle assembly is reduced to bcc-Fe nanoparticle assembly, as confirmed by XRD shown in Figure 2F. The reduction leads to the drastic increase in σ_s to 186 emu/g, a value close to 210 emu/g of bulk Fe. Magnetic measurements show that all as-synthesized Fe_3O_4 nanoparticles are superparamagnetic at room temperature.[17]

We have reported that high-temperature reaction of $Fe(acac)_3$ in the presence of alcohol, oleic acid, and oleylamine can be used to produce size-controlled monodisperse Fe_3O_4 nanoparticles. Further studies show that the synthesis is not limited to simple iron oxide nanoparticles but can be extended to various types of ferrite nanoparticles as well. The detailed studies on size-controlled synthesis, size-dependent magnetic properties of various iron-based nanoparticles, and their potential applications are underway.

Acknowledgment. H.Z. thanks the support by Louisiana Tech University and DoD/DAPRA through ARO under Grant No. DAAD 19-01-1-0546.

References

(1) Cornell, R. M.; Schwertmann, U. *The Iron Oxides: Structure, Properties, Reactions, Occurrence and Uses*; VCH: New York, 1996, pp28−29.

(2) (a) Verwey, E. J. W. *Nature* **1939**, *144*, 327. (b) Coey, J. M. D.; Berkowitz, A. E.; Balcells, L. I.; Putris, F. F.; Parker, F. T. *Appl. Phys. Lett.* **1998**, *72*, 734. (c) Soeya, S.; Hayakawa, J.; Takahashi, H.; Ito, K.; Yamamoto, C.; Kida, A.; Asano, H.; Matsui, M. *Appl. Phys. Lett.* **2002**, *80*, 823.

(3) Raj, K.; Moskowitz, R. *J. Magn. Magn. Mater.* **1990**, *85*, 233.

(4) Fu, L.; Dravid V. P.; Johnson, D. L. *Appl. Surf. Sci.* **2001**, *181*, 173.

(5) (a) Oswald, P.; Clement, O.; Chambon, C.; Schouman-Claeys, E.; Frija, G. *Magnetic Resonance Imaging* **1997**, *15*, 1025. (b) Kim, D. K.; Zhang, Y.; Kehr, J.; Klason, T.; Bjelke, B.; Muhammed, M. *J. Magn. Magn. Mater.* **2001**, *225*, 256.

(6) Jordan, A.; Scholz, R.; Wust, P.; Fahling, H.; Felix, R. *J. Magn. Magn. Mater.* **1999**, *201*, 413.

(7) (a) Kang, Y. S.; Risbud, S.; Rabolt, J. F.; Stroeve, P. *Chem. Mater.* **1996**, *8*, 2209. (b) Hong, C.-Y.; Jang, I. J.; Horng, H. E.; Hsu, C. J.; Yao, Y. D.; Yang, H. C. *J. Appl. Phys.* **1997**, *81*, 4275. (c) Fried, T.; Shemer, G.; Markovich, G. *Adv. Mater.* **2001**, *13*, 1158.

(8) Sapieszko, R. S.; Matijevic, E. *J. Colloid Interface Sci.* **1980**, *74*, 405.

(9) Vijayakumar, R.; Koltypin, Y.; Felner, I.; Gedanken, A. *Mater. Sci. Eng.* **2000**, *A286*, 101.

(10) Rockenberger, J.; Scher, E. C.; Alivisatos, P. A. *J. Am. Chem. Soc.* **1999**, *121*, 11595.

(11) Hyeon, T.; Lee, S. S.; Park, J.; Chung, Y.; Na, H. B. *J. Am. Chem. Soc.* **2001**, *123*, 12798.

(12) The mechanism leading to Fe_3O_4 under current reaction condition is not yet clear. Alcohol reduction of Fe(III) salt to Fe(II) intermediate followed by the decomposition of the intermediate at high temperature may be a possible route to Fe_3O_4. If $Fe(acac)_2$ is used, same product is obtained. No metallic Fe is detected in the final product.

(13) (a) Brown, K. R.; Natan, M. J. *Langmuir* **1998**, *14*, 726. (b) Jana, N. R.; Gearheart, L.; Murphy, C. J. *Chem. Mater.* **2001**, *13*, 2313. (c) Yu, H.; Gibbons, P. C.; Kelton, K. F.; Buhro, W. E. *J. Am. Chem. Soc.* **2001**, *123*, 9198.

(14) LaMer, V. K.; Dinegar, R. H. *J. Am. Chem. Soc.* **1950**, *72*, 4847.

(15) Watzky, M. A.; Finke, R. G. *J. Am. Chem. Soc.* **1997**, *119*, 10382.

(16) Klug, H. P.; Alexander, L. E. *X-ray Diffraction Procedures for Polycrystalline and Amorphous Materials*; John Wiley & Sons: New York, 1962; pp 491−538.

(17) Magnetic measurements were carried out using a superconducting quantum interference device with a field up to 7 T and temperatures 4−400 K.

JA026501X